Synthesis and Characterization of Calcium Hydroxyzincate Using X-ray Diffraction, FT-IR Spectroscopy, and Scanning Force Microscopy

Tien-Chih Lin, M. Yousuf A. Mollah, Rajan K. Vempati, and David L. Cocke*

Gill-Chair of Analytical Chemistry, Lamar University, Beaumont, Texas 77710

Received June 12, 1995. Revised Manuscript Received August 17, 1995[⊗]

Since calcium hydroxyzincate (CHZ) has been found to be central to the mechanism of Zn retardation of cement setting, pure samples of calcium hydroxyzincate (CHZ) have been prepared to provide pristine samples for characterization and to provide insight into the mechanism of its crystal growth. X-ray diffraction (XRD), Fourier transform infrared spectroscopy (FT-IR), and scanning force microscopy (SFM) have been used to provide structural, molecular, and morphological characteristics, respectively. The XRD results of the compound are in agreement with literature data which corresponds to the molecular formula $CaZn_2(OH)_6 \cdot 2H_2O$. The FT-IR results delineate the O–H stretching vibrations due to discrete noninteracting OH groups on the surface of CHZ. An idealized model structure is proposed to identify the positions and chemical environments of the discrete noninteracting OH groups in the hydroxylated zincate compound. The SFM images of CHZ crystals are presented, and these images provide information on growth mechanisms of this compound in a liquid. It is proposed that the growth of CHZ is initiated with the formation of surface nuclei, which quickly grow and coalesce to form layers across the surface. Some features characteristics of spiral dislocation was also observed on certain crystal surface. The mechanism of the formation of $CaZn_2(OH)_6 \cdot 2H_2O$ is discussed.

Introduction

The formation of calcium hydroxyzincate (CHZ) plays an important role in the retardation of cement hydration.[1–5] It also plays a role in slowing anode degradation in Zn/NiOOH batteries[6,7] and in the passivation of galvanized metal corrosion either in cement paste[8] or in alkaline solutions.[9] Arliguie et al.[3,4] have discussed the mechanism of formation of this passivating product, while Blanco et al.[9] reported the solution conditions that critically control the mechanism of reactions leading to this compound.

The crystal structure of CHZ has been reported by Lieber et al.[10] Several authors have studied the physicochemical properties,[11] the formation and decomposition kinetics,[12,13] morphology, and cell parameters[10,14] of CHZ. However, in a continuing research program to determine the speciation of priority metal pollutants in cementitious solidification/stabilization systems[15] results have been obtained which demonstrate that upon mixing of Zn^{2+} solutions with cement, an amorphous layer of zinc hydroxide precipitates on the surface of anhydrous cement particles. The zinc hydroxy complexes subsequently react with calcium hydroxide to produce $CaZn_2(OH)_6 \cdot 2H_2O$ (CHZ) to passivate the hydration reactions. The probable pH-dependent reactions leading to the formation of CHZ have also been reported elsewhere.[16] The concentration of Ca^{2+} ions in this system is a major controlling factor, and if there is a sufficient amount of Ca^{2+} ions in solution, either $Zn(OH)_2$ or ZnO will finally be transformed into CHZ.[9,17] The pH of the reaction medium also plays a critical role in the growth of CHZ crystals in the system, and once this compound is formed further increase of the pH does not affect the stability of the layers of CHZ.[17]

However, to better understand the growth mechanism and layered structure of CHZ, we have characterized this compound by X-ray diffraction (XRD) and Fourier transform infrared spectroscopy (FT-IR), and for the first time report its scanning force microscopic (SFM) images. We have systematically studied the thin films of CHZ to obtain morphological and structural information. Scanning force microscopy (SFM), also known as atomic force microscopy (AFM), is one of the unique surface analytical techniques that can provide three-dimensional information for the surface structure and allows in situ investigations of crystal growth and

[⊗] Abstract published in *Advance ACS Abstracts,* September 15, 1995.

(1) Lieber, W. *Zement-Kalk-Gips.* **1967**, *20*, 91.
(2) Lieber, W.; Gebauer, J. *Zement-Kalk-Gips.* **1969**, *22*, 161.
(3) Arliguie, G.; Ollivier J. P.; Grandet, J. *Cement Concrete Res.* **1982**, *12*, 79.
(4) Arliguie, G.; Grandet, J. *Cement Concrete Res.* **1990**, *20*, 517.
(5) Mollah, M. Y. A.; Parga, J. R.; Cocke, D. L. *J. Environ. Sci. Health Part A* **1992**, *27*(6), 1503.
(6) McBreen, J. *J. Electrochem. Soc.* **1972**, *111*, 1620.
(7) McBreen, J.; Cairns, E. J. *Advances in Electrochemistry and Electrochemical Engineering*; John Wiley and Sons Inc.: New York, 1978; Vol. 11, p 273.
(8) Duval, R.; Arliguie, G. *Mem. Sci. Rev. Metall.* **1974**, *71*(11), 5.
(9) Blanco, M. T.; Andrade, C.; Macias, A. *Br. Corros. J.* **1984**, *19*(1), 41.
(10) Liebau, F.; Amel-Zadeh, A. *Kristall Technik.* **1972**, *7*(1–3), 221.
(11) Sharma, R. A. *J. Electrochem. Soc.: Electrochem. Sci. Technol.* **1986**, *113*(11), 2215.
(12) Wang, Y.-M. *J. Electrochem. Soc.* **1990**, *137*(9), 2800.
(13) Inagaki, M.; Yamashita, Y. *J. Ceram. Soc. Jpn. Int. Ed.* **1987**, *95*, 329.
(14) Diehl, R.; Carpentier, C. D. *Nature Phys. Sci.* **1971**, *229*, 184.
(15) Cocke, D. L.; Mollah, M. Y. A. *Chemistry and Microstructure of Solidified Waste Forms*; Spence, R. D., Ed.; Lewis Publishers: Boca Raton, FL, 1993; pp 187–243.
(16) Mollah, M. Y. A.; Vempati, R. K.; Lin, T.-C.; Cocke, D. L. *Waste Management,* in press.
(17) Macias, A.; Andrade, C. *Br. Corros. J.* **1983**, *18*, 82.
(18) Vempati, R. K.; Cocke, D. L. *Proceeding of the XVth International Soil Science Society on Applications of Scanning Force Microscopy to Soil Minerals*; Acapulco, Mexico, July 1994.

0897-4756/95/2807-1974$09.00/0

Table 1. X-ray Powder Diffraction Data of Calcium Hydroxyzincate

Liebau and Amel-Zadch[a]			this study		
d spacing (Å)	intensity (%)	[*hkl*][b]	*d* spacing (Å)	intensity (%)	2*q*
6.237	80.0	100	6.170	89.1	14.3
5.008	90.0	011	4.977	1.9	17.8
4.116	80.0	120	4.099	1.4	21.7
3.926	80.0	021	3.916	0.9	22.7
3.560	70.0	121	3.558	0.7	25.0
3.123	90.0	200	3.104	100.0	28.7
2.881	100.0	131	2.878	1.7	31.0
2.814	70.0	022	2.809	1.6	31.8
2.706	50.0	220	2.702	1.1	33.1
2.454	60.0	$\bar{2}11$	2.454	3.0	36.6
2.388	50.0	$\bar{1}02$	2.382	0.6	37.7
2.322	10.0	231	2.328	0.4	38.6
2.295	20.0	212	2.291	0.5	39.3
2.157	40.0	222	2.150	0.4	42.0
2.079	20.0	$\bar{2}31$	2.077	4.0	43.5
2.043	40.0	310	2.043	0.9	44.3
1.946	40.0	320	1.942	2.3	46.7
1.820	70.0	331	1.819	1.8	50.1
1.739	30.0	$\bar{3}21$	1.737	1.3	52.7
1.658	30.0	340	1.655	0.6	55.5
1.577	60.0	411	1.574	2.7	58.6

[a] Reference 10. [b] [*hkl*] means Miller indices.

dissolution in solutions down to atomic resolution.[18] Furthermore, very limited discussion on the infrared spectra of CHZ has been reported in the literature.[9] We present here a detailed discussion of the FT-IR spectra of this compound.

Experimental Section

Synthesis of Calcium Hydroxyzincate. Analytical grade chemicals received from Fisher Scientific Co. (Fair Lawn, NJ) were used in this study. Calcium hydroxyzincate was synthesized following the method reported by Sharma.[11] According to this method 2.5 g of ZnO was dissolved in 250.0 mL of 20% (w/w) KOH solution and 25.0 g of pure $Ca(OH)_2$ dissolved in 36.5 g of deionized water was slowly added to this mixture with constant stirring. The amount of water and zinc oxide required to react with 25.0 g of calcium hydroxide was calculated based on the molecular formula of CHZ. Additional amount of ZnO (54.93 g) was then slowly added to the mixture and stirred for 24 h. After that, the CHZ crystals were allowed to settle, and the supernatant liquid was decanted off. The CHZ was washed with deionized water until the pH of the solution became ~7.0. The compound was dried overnight at 325 K and stored for analyses.

Characterization of CHZ. *X-ray Diffraction (XRD).* The XRD analyses were performed using Cu Kα radiation (35 kV and 25 mA) on a Scintag XDS 2000 diffractometer equipped with a graphite monochromator. Calcium hydroxyzincate was pulverized using a mortar and pestle and then filled into a ring-shaped hollow aluminum holder. The holder contains glass slide that has a rectangular hollow area for holding powdered samples. The CHZ samples were gently pressed with a glass slide into the rectangular area. The XRD scan was run at 0.02° steps and 15 s counting time.

Fourier Transform Infrared (FT-IR). Diffuse reflectance infrared spectra of the powdered CHZ samples were recorded using a Perkin-Elmer System 2000 FT-IR spectrometer. Pure CHZ (10 mg) was mixed with FT-IR grade KBr powder and filled into a hollow steel holder. The sample was scanned 25 times in the region 4000−400 cm^{-1}, and the average spectrum was corrected using the diffuse reflectivity spectrum of KBr run under identical conditions. Band positions were determined by fitting Gaussian bands to the Kubelka−Munk (KM) function.

Surface Imaging by Scanning Force Microscopy (SFM). The surface images of CHZ were scanned using the TopoMetrix TMX 2000 scanning probe microscope system. Since it is extremely difficult to image powdered samples because the sample could adhere on the cantilever tip resulting in a poor image, a thin film was formed on a piece of silica (100) wafer. A small amount of CHZ powder was taken into a glass vial and filled with deionized water. The vial was shaken vigorously in an end-over-end fashion so that the powder was suspended in water, and the mixture sonicated for 5 min to evenly disperse the crystals in water. One drop of this suspension was then gently placed on a piece of silica (100) wafer and allowed to air-dry before taking the images. The thickness of the film formed on the silica wafer was adjusted by trial and error after repeated dilution of the suspension until a good image was recorded. The sample was imaged with a 75 μm scanner, and sufficient time was allowed to eliminate thermal and mechanical drifts so that good quality images were obtained. All samples were imaged in air and at ambient temperature.

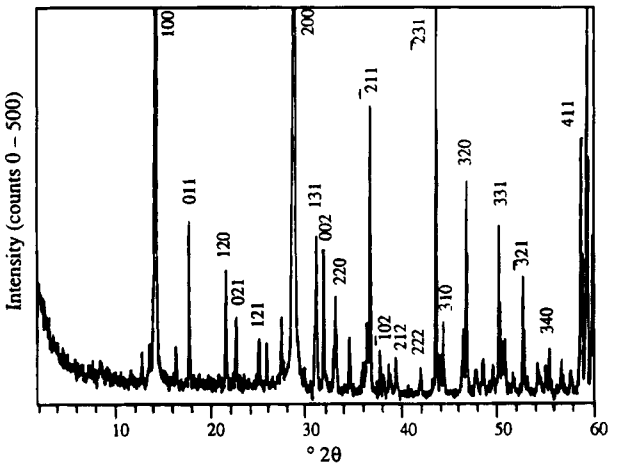

Figure 1. X-ray powder diffraction pattern of calcium hydroxyzincate.

Results and Discussion

XRD. The X-ray diffraction data of the compound are presented in Table 1, and the corresponding diffractogram is shown in Figure 1. The single crystal XRD data of CHZ reported by Liebau et al.[10] are also included in Table 1 for comparison. Miller indices assigned to the single crystal XRD data are listed in the table for reference. It can be seen from Table 1 that as many as 20 out of a total of 26 peaks are in good agreement with the single crystal XRD data reported by others[10,19] which correspond to the formula $CaZn_2(OH)_6 \cdot 2H_2O$ for CHZ. The crystal structure and the cell parameters have also been reported by Liebau et al.[10] A close examination of the peak positions, however, reveals that in some cases the peak positions have been slightly shifted. For example, peaks corresponding to *d* spacing 6.170, 4.977, 4.099, 3.916, and 3.104 Å appear at slightly different positions as compared with the data reported by Liebau et al.[10] Nevertheless, the XRD results clearly indicate that we were able to synthesize a pure sample of the compound $CaZn_2(OH)_6 \cdot 2H_2O$.

FT-IR Analyses. A typical FT-IR spectrum of CHZ is shown in Figure 2. The FT-IR bands due to different vibrational modes were characterized by comparing with analogous groups in other compounds and ions reported in the literature.[20] The zinc ions are tetrahedrally coordinated by four hydroxyl groups in CHZ,[10] and these tetrahedral XY_4 molecules are expected to exhibit four

(19) Berry, L. G., Ed. *Inorganic Index to the Powder Diffraction File. Joint Committee on Powder Diffraction Standards*; Pennsylvania, 1974; reference pattern no. 24-222 of JCPDS.

(20) Nakamoto, K. *Infrared and Raman Spectra of Inorganic and Coordination Compounds*, 3rd ed.; John Wiley & Sons: New York, 1978.

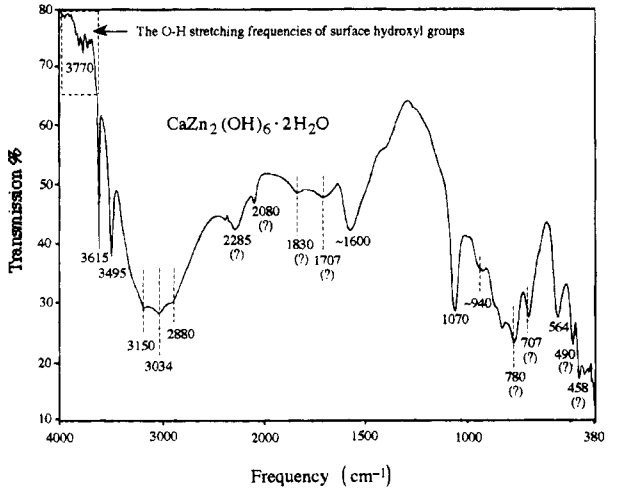

Figure 2. FT-IR spectrum of calcium hydroxyzincate.

normal modes of vibrations (ν_1 to ν_4). Only ν_3 and ν_4 are infrared active. The ν_3 $Zn(OH)_4^{2-}$ band at 564 cm^{-1} is assigned to the Zn−O vibration in the skeleton of ZnO_4. The ν_4 $Zn(OH)_4^{2-}$ band at 300 cm^{-1} is out of range of the scanned frequencies in the spectrum.[21] The band at 1070 cm^{-1} is attributed to the Zn−O−H bending vibration.

The hydroxo complex exhibits the MOH (M = metal atom) bending mode below 1200 cm^{-1}.[20,22] The OH group can also form a bridge between two metal atoms as shown below: Hence, the band at ~940 cm^{-1} is

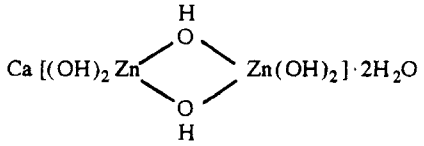

assigned to bridging O−H bending vibration.[23] Lattice water generally absorbs in the range 3550−3200 cm^{-1} due to the antisymmetric and symmetric O−H stretching vibrations ($\nu_1 + \nu_3$). Also, the H−O−H bending mode (ν_2) will exhibit a band at 1630−1600 cm^{-1}. The O−H stretching bands appear at lower frequencies when hydroxyl ion $[OH]^-$ forms hydrogen bonding with lattice water within the crystal structure. The bands at 2880, 3034, and 3150 cm^{-1} are attributed to the O−H stretching modes ($\nu_1 + \nu_3$) of OH_2 in CHZ. The HOH bending mode (ν_2) of lattice water in CHZ appears at ~1600 cm^{-1}, which is in good agreement with similar bands reported for other hydrated compounds.[24]

The hydroxyl ions $[OH]^-$ are characterized by sharp bands appearing between 3700 and 3500 cm^{-1}. The positions of the OH^- ions and their chemical environments may be schematically represented as

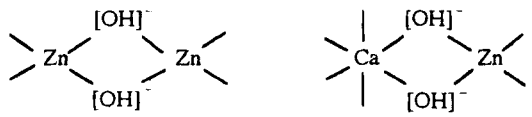

Therefore, two sharp bands at 3495 and 3615 cm^{-1} are assigned to the O−H stretching vibrations of these two hydroxyl groups.

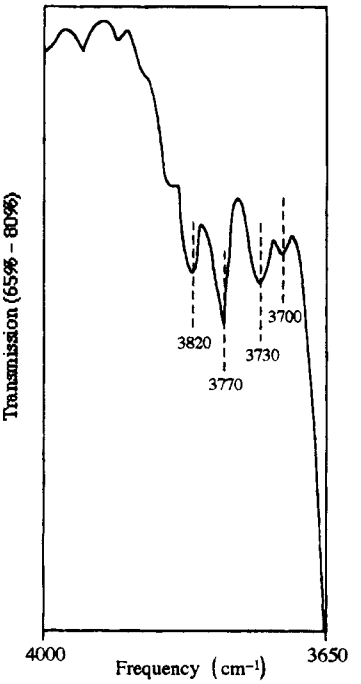

Figure 3. FT-IR spectrum of calcium hydroxyzincate in the region of OH stretching vibrations due to the surface hydroxyl groups.

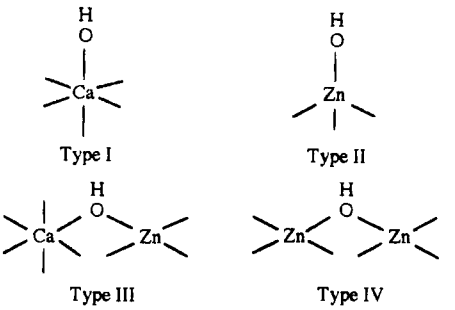

Figure 4. Types of hydroxyl groups on the surface of calcium hydroxyzincate.

The bands at 3700, 3730, 3770, and 3820 cm^{-1} are assigned to O−H stretching vibrations due to discrete noninteracting OH groups on the surface of CHZ. These bands can be seen more clearly in the computer-aided expanded spectrum shown in Figure 3. The positions and chemical environments of the discrete noninteracting OH groups may be shown by idealized model structures shown in Figure 4. An analogous case has been noted on the surface of γ-alumina.[25,26] There are four different types of OH groups (types I−IV) expected on the surface of CHZ. The occurrence and number of each type depends on the relative contribution of specific crystal faces or surface defect sites. The surface OH groups may be on (i) the octahedral site of calcium ions (type I), (ii) the tetrahedral site of zinc ions (type II), (iii) the bridging site between calcium and zinc (type III) or (iv) the bridging site between two zinc ions (type IV). The various types of OH groups are expected to have varying chemical properties. The basicity of the OH group decreases from type I to type IV. The more basic type should have higher vibrational absorption frequency. As a result, the O−H stretching bands at 3820, 3770, 3730, and 3700 cm^{-1} are assigned to the structures represented by types I−IV of surface OH

(21) Lippincott, E. R.; Psellos, J. A.; Tobin, M. C. *J. Chem. Phys.* **1952**, *20*, 536.
(22) Maltese, M.; Orville-Thomas, N. J. *J. Inorg. Nucl. Chem.* **1967**, *29*(10), 2533.
(23) Ferraro, J. R.; Walker, W. R. *J. Inor. Chem.* **1965**, *4*(10), 1382.
(24) Miller, F. A.; Wilkins, C. H. *Anal. Chem.* **1952**, *24*, 1253.
(25) Peri, J. B.; Hannan, R. B. *J. Phys. Chem.* **1960**, *64*, 1526.
(26) Peri, J. B. *J. Phys. Chem.* **1965**, *69*, 220.

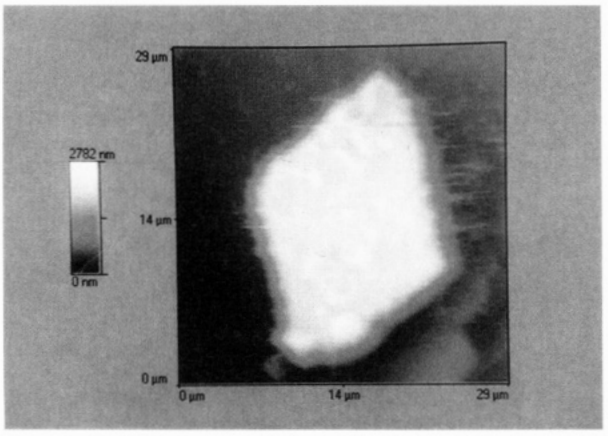

Figure 5. SFM image of calcium hydroxyzincate single crystal.

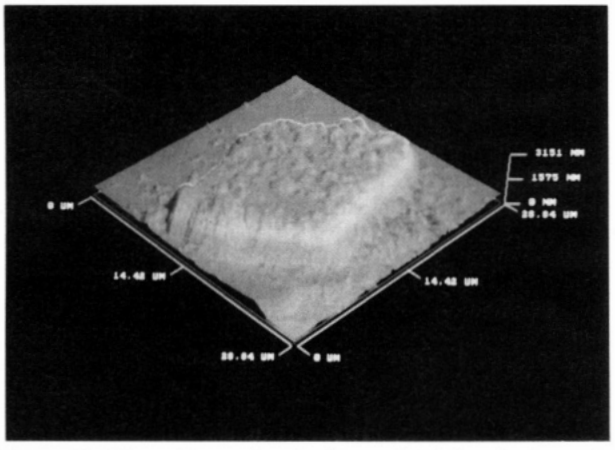

Figure 6. Three-dimensional picture of calcium hydroxyzincate single crystal.

groups, respectively. The interpretation of FT-IR results presented above strongly supports the structure of CHZ reported by Liebau et al.[10] The bands appearing at 458, 707, 780, 1707, 1830, 2080, and 2285 cm^{-1} (Figure 2) cannot be assigned on the basis of present experiment only. Further experiments are needed to identify these bands. However, the O−H stretching bands due to surface OH groups and hydroxyl ions in this study are in good agreement with those reported by Cocke et al.[5] from FT-IR investigation of zinc-doped cement.

SFM Imaging. The surface images of CHZ were obtained by ex-situ method using the scanning force microscope. The SFM image of a single CHZ crystal is shown in Figure 5 and the three-dimensional (3D) image of the corresponding single crystal is presented in Figure 6. This crystal has a length of ~25 μm, width of ~16 μm, and thickness of ~1 μm. Close examinations of these images demonstrate that this crystal possesses a well defined monoclinic structure ($\alpha \neq \beta \neq \chi$, $\alpha = \gamma = 90°$, $\beta \neq 90°$). The surface topography of the crystals imaged by SFM reveals the growth mechanism of CHZ. A zoom image on the surface of a single particle (Figure 5) is presented in Figure 7. This image exemplifies the polynuclear or birth-and-spread models of layer growth[27,28] of this compound in a liquid matrix.

Close examination of Figure 7 reveals that the growth of CHZ is initiated with the formation of surface nuclei.

(27) Ohara, M.; Reid, R. C. *Modeling Crystal Growth Rates from Solution*; Prentice-Hall: Englewood Cliffs, NJ, 1973.
(28) Nielsen, A. E. *J. Cryst. Growth* **1984**, *67*, 289.

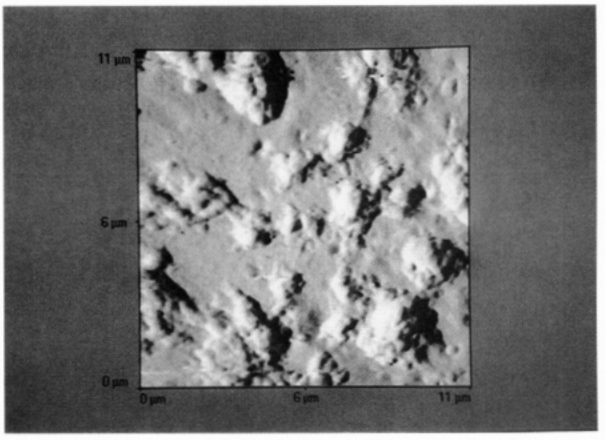

Surface Finish Measurements	
Area = 5µm x 5µm	
R_a = 102.99 NM	Z_{AVG} = 202.80 NM
R_{rms} = 133.10 NM	Z_{MAX} = 699.06 NM

Figure 7. SFM image (shaded) of surface nuclei and coalescent forms of nuclei on calcium hydroxyzincate single crystal.

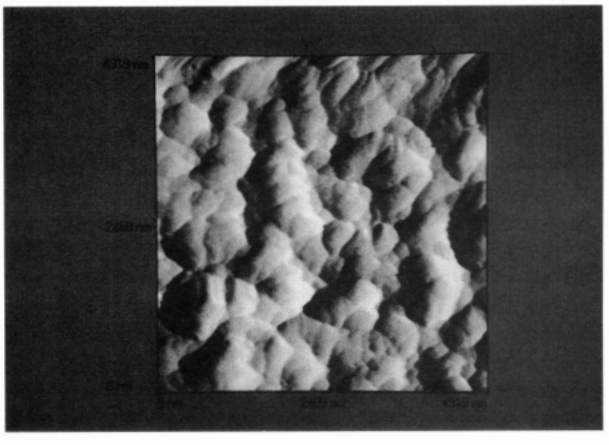

Surface Finish Measurements	
Area = 5µm x 5µm	
R_a = 60.89 NM	Z_{AVG} = 220.14 NM
R_{rms} = 79.70 NM	Z_{MAX} = 506.08 NM

Figure 8. SFM image (shaded) of new smoother surface formed by the spreading of surface nuclei on calcium hydroxyzincate.

The nuclei that grow on the preexisting surface have a rhombohedral-like form. Following the surface nucleation stage, these nuclei quickly grow and coalesce with layer growth proceeding across their larger unified surface. Measurements of the smallest nucleus to larger coalescent regions indicate heights of 65−560 nm. As the precipitation continues, the nuclei and the larger coalescent forms blend to give a new smoother surface as shown in Figure 8. The engineering parameters used to describe surface roughness are also given in Figures 7 and 8. For the area of 5 μm × 5 μm, the R_{rms} values are 133.10 and 79.70 nm for Figures 7 and 8, respectively. The surface morphology shown in Figure 8

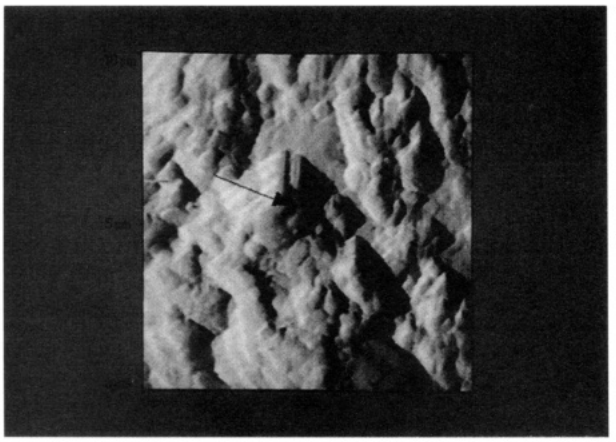

Figure 9. SFM image (shaded) of the growing spiral on the surface of calcium hydroxyzincate.

clearly indicates a smoother surface. However, on surfaces of a relative large area, many critical nuclei may form simultaneously, even one upon another,[29] according to the polynuclear or birth and spread model described by Hillig[30] and Nielsen.[31]

In addition to surface nucleation mechanism, feature characteristics of spiral dislocation was also found on another crystal surface (Figure 9). This is consistent with the crystal growth theory that the rate of crystal growth is the sum of the two individual process (surface nucleation and spiral dislocation) with the faster one dominating.[28] At sufficiently high supersaturation, surface nucleation may dominate the overall growth rate. However, at very low supersaturation (near-equilibrium condition), since surface nucleation is extremely slow, the growth rate of a surface with a screw dislocation will be determined mainly by a spiral dislocation mechanism. No matter what determine the rate of crystal growth, the layer-by-layer structure in a crystal can be created by the spreading of monolayer steps. The multilayer steps can be formed after the displacement between two multilayers, which can be seen clearly in Figure 10.

On the basis of the framework constructed by the extension of unit cell[14] and the molecular structure of CHZ reported by Liebau et al.,[10] we believe that CHZ has a perfect cleavage parallel (001), caused by its layered structure. The structure consists of layers of $Zn_2(OH)_6^{2-}$ (a bridge form of two tetrahedrons), which are bound together by Ca^{2+} cations. Water molecules are arranged between these layers. A perfect cleavage occurs along the water layers parallel to (001). A similar structure, a cleavage parallel (010) shown in gypsum crystal, has been reported by Cole and Lancucki.[32] Therefore, the crystal growth of CHZ on a (001) surface is expected to be dominated by the growth in the [100] and [010] directions. The difference of the growth rate in [100] direction and in [010] direction cannot be determined by the present experiment. However, this can be investigated by further experiments on direct in situ observations of CHZ growth using SFM with a fluid cell, which allows real-time imaging in an aqueous environment.

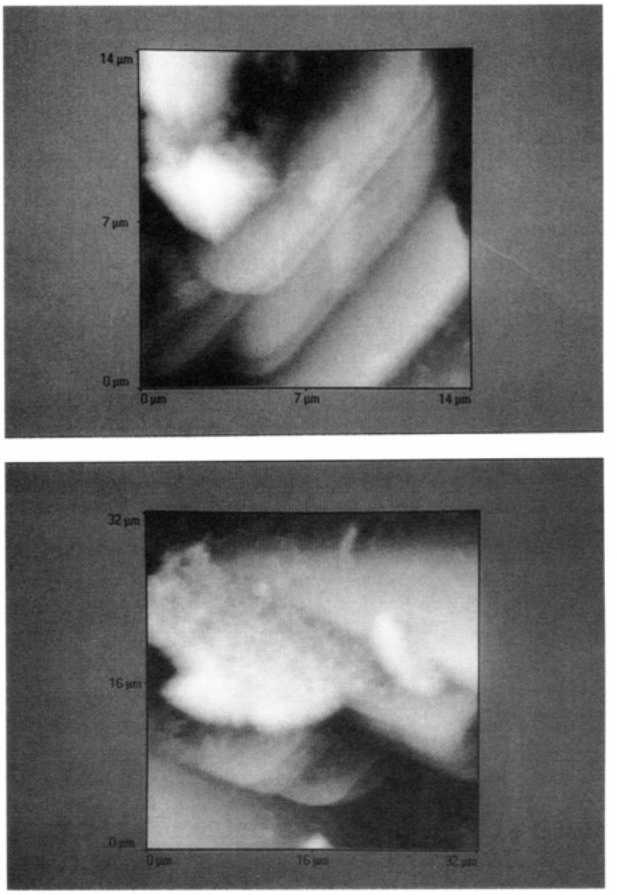

Figure 10. SFM images of the layer-by-layer growth on calcium hydroxyzincate.

Conclusions

The preparation of CHZ is accomplished by careful manipulation in aqueous solutions and provides material that can be characterized by modern materials characterization methods. The results presented in this article clearly demonstrate that the formation of calcium hydroxyzincate crystal is preceded by surface nucleation, and once the critical nucleus is formed it spontaneously spreads across the entire surface. Additional features characteristics of spiral dislocation was also observed on certain crystal surfaces. The SFM images presented in this article provides valuable information on (1) the surface morphology of CHZ crystals and (2) the layer-by-layer crystal growth features on the edges, which cannot be otherwise obtained by SEM.[9,15] The FT-IR results have delineated the nature and chemical environments of the hydroxyl groups in the zincate structure. The results of these characterizations will aid in identifying and characterizing CHZ in complex systems such as cement, electrodes, environmental precipitates, in corrosion prevention layers.

Acknowledgment. We thank the Gulf Coast Hazardous Substance Research Center, Lamar University, Beaumont, for the funding to support this work. Partial support for this work came from the Welch Foundation, Houston, TX. We acknowledge NASA-Johnson Space Center, Houston, TX, and Professor Loeppert of Texas A&M University for the generous use of their instruments.

CM950261L

(29) Zhang, J.-W.; Nancollas, G. H. *Reviews in Mineralogy*; Hochella Jr., M. F.; White, A. F., Eds.; The Mineralogical Society of America: 1990; Vol. 23, p 377.
(30) Hillig, W. B. *Acta Metall.* **1966**, *14*, 1868.
(31) Nielsen, A. E. *Croat. Chem.* Acta. **1980**, *53*, 255.
(32) Cole, W. F.; Lancucki, C. J. *Acta Crystallogr.* **1974,** *B30*, 921.